Vacuum 85 (2010) 89–94

Contents lists available at ScienceDirect

Vacuum

journal homepage: www.elsevier.com/locate/vacuum

Influence of CH_4 fraction on the composition, structure, and internal stress of the TiCN coatings deposited by LAFAD technique

Y.H. Cheng*, T. Browne, B. Heckerman

American Eagle Instruments, Inc., 6575 Butler Creek Rd, Missoula, MT 59808, United States

ARTICLE INFO

Article history:
Received 22 December 2009
Received in revised form
7 April 2010
Accepted 11 April 2010

Keywords:
Filtered cathodic arc
TiCN coating
Structure
Internal stress

ABSTRACT

TiCN coatings were deposited using a large area filtered arc deposition (LAFAD) technique from Ti targets in a mixture of N_2 and CH_4 gases. CH_4 fraction was varied from 0 to 50% to change the C content in the coatings. Scanning electron microscopy (SEM), x-ray photoelectron spectroscopy (XPS), x-ray diffraction (XRD), and substrate bending method were used to characterize the dependence of the CH_4 fraction on the surface morphology, composition, bonding structure, crystalline structure, and internal stress in the deposited coatings. It was found that TiCN coatings consist of nano-sized clusters and the cluster size increases with CH_4 fraction. XPS results show that with increasing CH_4 fraction, the N content in the coatings decrease continuously, the C content increases to 9.3 at.% at a CH_4 fraction of 30% followed by a slight decrease with the additional increase in the CH_4 fraction. With an increase of the C content in the coatings, there is a decrease in the Ti–N bonding content and an increase in the Ti–C and C–N bonding contents in the coatings. XRD results indicate that with increasing CH_4 fraction, the growth orientation of the TiCN coatings changes from (111) to (220) preferred orientation. The TiN (220) peak shifts to a lower diffraction angle, and the grain size decreases continuously. The internal stresses in all TiCN coatings are compressive and increase linearly with increasing C content in the coatings. The decrease in the grain size and the increase in the C content correspond to the continuous increase in the internal stress in the coatings.

1. Introduction

Titanium carbonitride (TiCN) coatings attract great attention due to their combined high hardness, high toughness, low friction coefficient, excellent wear and abrasion resistance [1–5]. TiCN coatings are widely used in many industries where high wear resistant surfaces are needed. Generally, TiCN coatings have been deposited by CVD method [6]. However, the high deposition temperature (1000 °C) limits the selection of the substrate material. To reduce the deposition temperature, various PVD techniques, such as magnetron sputtering [7–9], laser ablation [10], cathodic arc [2,11], and filtered cathodic arc [12,13], have been developed. Among them, filtered cathodic vacuum arc technology is the most attractive due to the high ionization rate, high ion energy, and high deposition rate, which enables the deposition of high quality coatings with high adhesion at low temperatures. In our previous paper [13], we reported the successful deposition of TiCN coatings using a large area cathodic vacuum arc deposition (LAFAD) technology with Ti targets at a mixture of N_2 and CH_4 gases at a temperature of 350 °C and pressure of 0.02 Pa.

As TiCN coatings are a solid solution of TiN and TiC phases, the variation in the carbon content in the coatings causes significant changes in their crystalline structure, bonding structure, as well as the internal stress. Generally, TiCN lattice parameter values are located between the lattice parameter values of TiN and TiC, and increase with increasing C content in the coatings [8]. The growth orientation of the TiCN coatings is strongly dependent on the deposition method and C content in the coatings. Senna [8] discovered that TiCN coatings deposited by magnetron sputtering ion plating exhibit a (200) preferred orientation. Huang [12] reported that all the TiCN coatings deposited by filtered cathodic arc exhibit a strong (111) preferred orientation, and the peak center shifts to lower Bragg angles with increasing C content in the coatings. Deng [14] found a continuous increase in the residual stress with increasing C/Ti ratio in the TiCN coatings deposited by magnetron sputtering. It is necessary to investigate the influence of the C content on the structure and internal stress of the TiCN coatings deposited by LAFAD.

In this study, TiCN coatings were synthesized by LAFAD technique from Ti targets under an atmosphere of a mixture of N_2 and CH_4 gases. The C content in the TiCN coatings was controlled by

* Corresponding author.
E-mail addresses: yh_cheng@yahoo.com, ycheng@am-eagle.com (Y.H. Cheng).

0042-207X/$ – see front matter © 2010 Elsevier Ltd. All rights reserved.
doi:10.1016/j.vacuum.2010.04.007

adjusting CH_4 fraction in the deposition chamber. The surface morphology, microstructure, crystalline structure, and internal stress in the deposited TiCN coatings were characterized by scanning electron microscopy (SEM), x-ray diffraction (XRD), x-ray photoelectron spectroscopy (XPS), and substrate bending method, respectively. The influence of the CH_4 fraction in the gas on the surface morphology, crystalline structure, composition, bonding structure, and internal stress in the TiCN coatings was systematically studied.

2. Experimental details

A LAFAD-1 surface engineering system was used to deposit TiCN coatings. The detailed description of the deposition system was published previously [15]. Briefly, this system consists of one dual filtered arc source, one rectangular plasma-guide chamber, one deposition chamber, auxiliary anodes, heating system, substrate bias system, and vacuum system. The dual filtered arc source consists of two primary cathodic arc sources utilizing round Ti targets, which are placed opposite to each other on the side walls of the plasma-guide chamber, surrounded by rectangular deflecting coils, and separated by an anodic baffle plate. The deposition temperature was controlled by heating elements and measured by a thermalcouple located at the top of the deposition chamber. The deposition zone for this system is approximately 500 mm in diameter $\times$ 300 mm high. 17-4 stainless coupons and 5 cm n-type (111) Si wafers with a resistivity and thickness of $<$0.005 Ohm cm and 279 $\pm$ 25 μm, respectively, were used as substrates for characterizing the surface morphology, bonding structure, crystalline structure and internal stress in the coatings, respectively. 17-4 stainless steel coupons were cut from φ12.5 mm bars, followed by grinding and polishing to a mirror finish surface with a surface roughness (RMS) of about 12 nm.

The substrates were ultrasonically cleaned and dried before loading into the deposition chamber. Before deposition, the coupons were subjected to Ar plasma cleaning at a pressure, temperature, bias, and time of 0.08 Pa, 350 °C, −250 V, and 15 min, respectively, followed by the Ti ion sub-implantation at a pressure, bias, and time of 0.02 Pa, 500 V, and 2 min. In order to improve the adhesion of the TiCN coatings, a Ti–TiN gradient multilayer with a thickness of about 200 nm was initially deposited onto the coupon surface. The gradient layer was deposited by gradually increasing N_2 content in a mixed N_2 and Ar atmosphere from 0 to 100%. After the deposition of the compositional gradient bonding layer, TiCN coatings with a thickness of 2.5 μm were deposited. The TiCN coatings were deposited at a temperature of 350 °C, pressure of 0.02 Pa, and a substrate bias of −40 V. To deposit TiCN coatings with different C content, the CH_4 fraction in the mixed CH_4 and N_2 gases was varied from 0 to 50%. The coatings with a CH_4 fraction of 5, 10, 20, 30, and 50% were denoted as TiC5N, TiC10N, TiC20N, TiC30N, and TiC50N, respectively.

The surface morphology of the TiCN coatings was observed using a Hitachi S-4700 field emission SEM at the EMtrix Electron Microscopy Center, the University of Montana. The SEM was operated at 20 kV. The phase structure and grain size of the TiCN nanocomposite coatings were studied using a Siemens D500 x-ray diffractometer with a Cu-K_α radiation source ($\lambda = 0.15406$ nm). The accelerating voltage and filament current were 40 kV and 30 mA, respectively.

The composition and bonding structure of the TiCN coatings were investigated using an XPS instrument (PHI Model 5600ci, Casa XPS Analytical Software). A monochromatic Al K_α x-ray source was used for all samples. The conditions used for the survey scans were as follows: energy range, 1100–0 eV; pass energy, 160 eV; step size, 0.7 eV; sweep time, 180 s; and x-ray spot size, 700 $\times$ 400 μm. For the high-resolution spectra, an energy range of 40–20 eV was used, depending on the peak being examined, with a pass energy of 10 eV and a step size of 0.05 eV.

The isotropic biaxial stress in the as-deposited TiCN coatings was determined by the radius of curvature technique which compares the curvatures of the bare silicon substrates and substrates coated with a film. The stress was given by Stoney's equation [16]:

$$\sigma = \frac{E_s t_s^2}{6(1-\nu_s)t_c}\left(\frac{1}{R_a} - \frac{1}{R_b}\right)$$

where E_s and ν_s are Young's modulus and Poisson's ratio for the substrate, t_s and t_c are the thickness of the substrate and coating, R_a and R_b are the spherical radius of curvature of the substrate after and before coating deposition, respectively.

The radius of the curvature of the Si wafer was measured by a contact skidless type surface profilometer (Veeco Dektak8). The stylus radius, stylus force, and scan length were set to 5 μm, 10 mg, and 25 mm, respectively. Before and after coating deposition, the radius of curvature of each Si wafer was measured at exactly the same location close to the wafer center. For each wafer, three measurements were conducted and their average is reported. The coating thickness was measured using a Calotester (CSM).

3. Results and discussions

Fig. 1 shows the typical SEM images of the (a) Ti10CN, (b) Ti20CN, (c) Ti 30CN, and (d) Ti50CN coatings deposited by LAFAD. As shown, TiCN coatings deposited at a CH_4 fraction of 10% are very smooth, and nano-sized clusters with a size of about 200–300 nm uniformly distributed in the matrix of the coatings. With the increase in the CH_4 fraction to 20%, the clusters become more obvious. Some facets could be distinguished from the cluster background. However, there is no significant change in the cluster size. At a CH_4 fraction of 30%, the density of the particles and defects increase, the cluster size increases to 250–800 nm, but the density of the cluster decreases remarkably. With the further increase in the CH_4 fraction to 50%, there is no significant change in the size and shape of the clusters. However, a considerable increase in the density of the clusters was observed.

The composition and bonding structure of the deposited TiCN coatings were characterized by XPS. In order to characterize the composition and the bonding structure of the TiCN coatings, high-resolution spectra of Ti 2*p*, N 1*s*, and C 1*s* were collected and fitted using Gaussian function. All spectra were calibrated using the adventitious C 1*s* peak with a fixed value of 284.6 eV. The background from each spectrum was subtracted and the area of under each peak was used to calculate the composition of the TiCN coatings using relative sensitivity factors from the manufacturer's handbook: Ti (1.798), N (0.477), and C (0.296).

Fig. 2 plots the C, Ti, and N content in the TiCN coatings as a function of CH_4 fraction in the gas. With increasing CH_4 fraction in the gas from 5 to 30%, C content in the coatings increases linearly from 2.8 to 9.3%, N content in the coatings decreases from 44 to 36.8 at.%. The further increase in the CH_4 fraction to 50% results in a slight decrease in the C and N content to 8.8 at.% and 36.4 at.%, respectively. Cathodic arc discharge produces large amounts of high energy ions and low energy electrons. The low energy electrons are attracted to the deposition chamber by an auxiliary anode. CH_4 and N_2 gases in the deposition chamber are ionized by these low energy electrons, which generate reactive CH_x^{n+} and N^+ ions in the chamber. The reaction of the CH_x^{n+} and N^+ ions with Ti^{n+} on the substrate surface produces TiCN coatings. With the increase in the CH_4 fraction in the chamber, more CH_x^{n+} ions and less N^+ ions

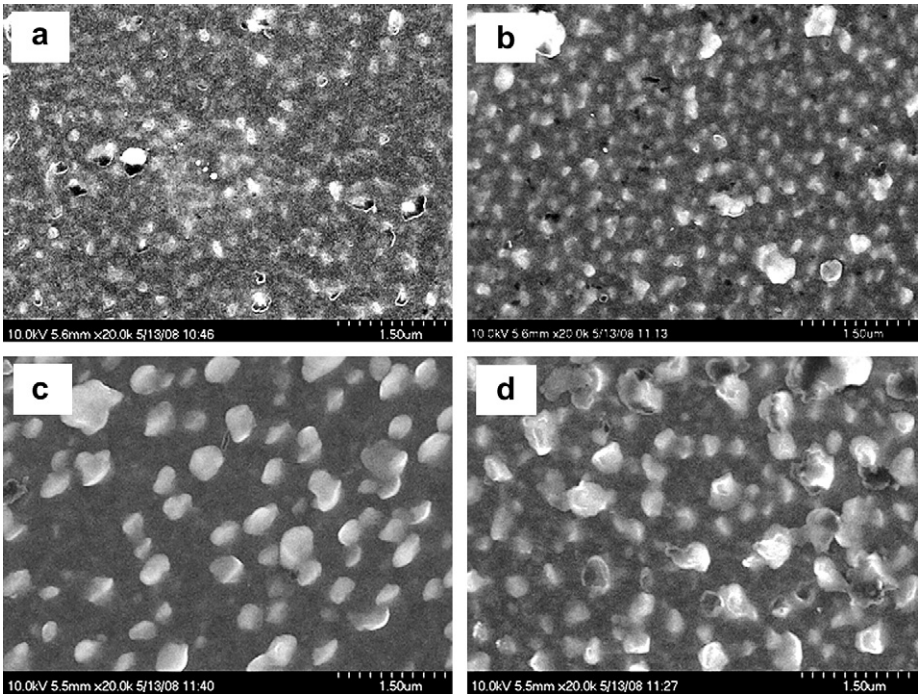

Fig. 1. SEM images of (a) Ti10CN, (b) Ti20CN, (c) Ti 30CN, and (d) Ti50CN coatings deposited by LAFAD.

are produced, and more C and less N atoms will be incorporated into the coating, corresponding to the increase and decrease in the C and N content in the coatings, respectively. In addition, H atoms were also incorporated into the coating during deposition. Due to the high deposition temperature (350 °C), those H atoms could diffuse and react to each other and form H_2. Our stress measurement results showed that high compressive internal stress exists in the TiCN coatings with high C content. The aggregation of the H_2 in the coatings could generate additional local internal stress. When the total local internal stress exceeds the Ti–C–N bonding strength, sub-micron sized cracks/defects will form.

It is interesting to note that the Ti content in the coatings increases slightly from 53.1 to 54.8 at.% with increasing CH_4 fraction from 5 to 50%. This may imply that adding CH_4 gas into the chamber decreases the reactivity of ions in the plasma, resulting in the incorporation of less C and N atoms into the coatings.

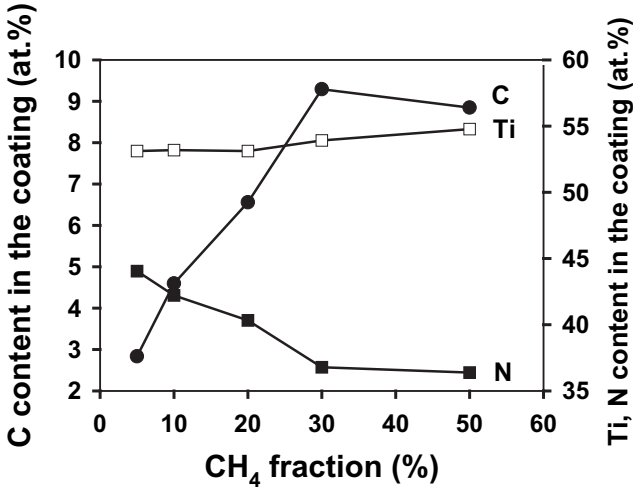

Fig. 2. Influence of CH_4 fraction on the C, Ti, and N content in the TiCN coatings.

Fig. 3 depicts the high-resolution Ti 2*p*, N 1*s*, and C 1*s* XPS spectra from the TiCN coatings with different C content, and the typical deconvolution results of the Ti 2*p*, N 1*s*, and C 1*s* XPS spectra from TiC5N coatings. All Ti 2*p* spectra consist of two main peaks at a binding energy of 455.0 and 460.9 eV, and two shoulder peaks at a binding energy of 457.1 and 463.2 eV. As we have already pointed out elsewhere [17], the first main peak and its shoulder peak are attributed to the $2p_{3/2}$ splitting, and the second main peak and its shoulder peak are their respective $2p_{1/2}$ splitting. The two main peaks correspond to TiN phase, while the two shoulder peaks could be a combination of the intermediate phases such as Ti_2O_3 or oxynitrides as suggested by some researchers [17], as well as the inherent satellite peaks of the two main peaks of the TiN phase.

All N 1*s* XPS spectra exhibit a slightly symmetric peak at 397.03 eV with a weak shoulder at 399.48 eV in the binding energy range of 395–402 eV. For the coatings deposited with a CH_4 fraction in the gases smaller than 20%, there is no significant change in the peak center (397.03–397.16 eV), but a further increase in the CH_4 fraction to 30% leads to a downshift of the peak center to 396.85 eV. Guemmaz et al. [18] also found that the binding energy of the N 1s spectra of the TiCN coatings was lower than that of the TiN coatings. The shoulder peak is associated with C(sp^2)–N bond as well as phyidine-like N containing ring. This indicates the existence of N–Ti bonds, N–C bonds, and N–O–Ti bonds in the TiCN coatings, but most of the N atoms in the coating are bonded to Ti atoms.

All the C 1*s* spectra consist of two peaks at the binding energy of 284.6 and 281.8 eV. The first peak is assigned to the C–C bonds which originates from the adventitious carbon. The second peak is very close to the C1*s* binding energy (281.9 eV) of Ti–C bonds, and can be assigned to the Ti–C bonds. As compared with the first peak, the second peak accounts for only a small fraction of the total C1*s* spectra, indicating that a small fraction of C atoms are bonded to Ti atoms, and most of the C atoms exist as amorphous carbon. With the increase in the CH_4 fraction, the intensity of both peaks increase but the intensity of the peaks at 284.6 increases faster. This implies that there exists a large amount of amorphous carbon in the TiCN coatings deposited with high CH_4 fraction. This will significantly

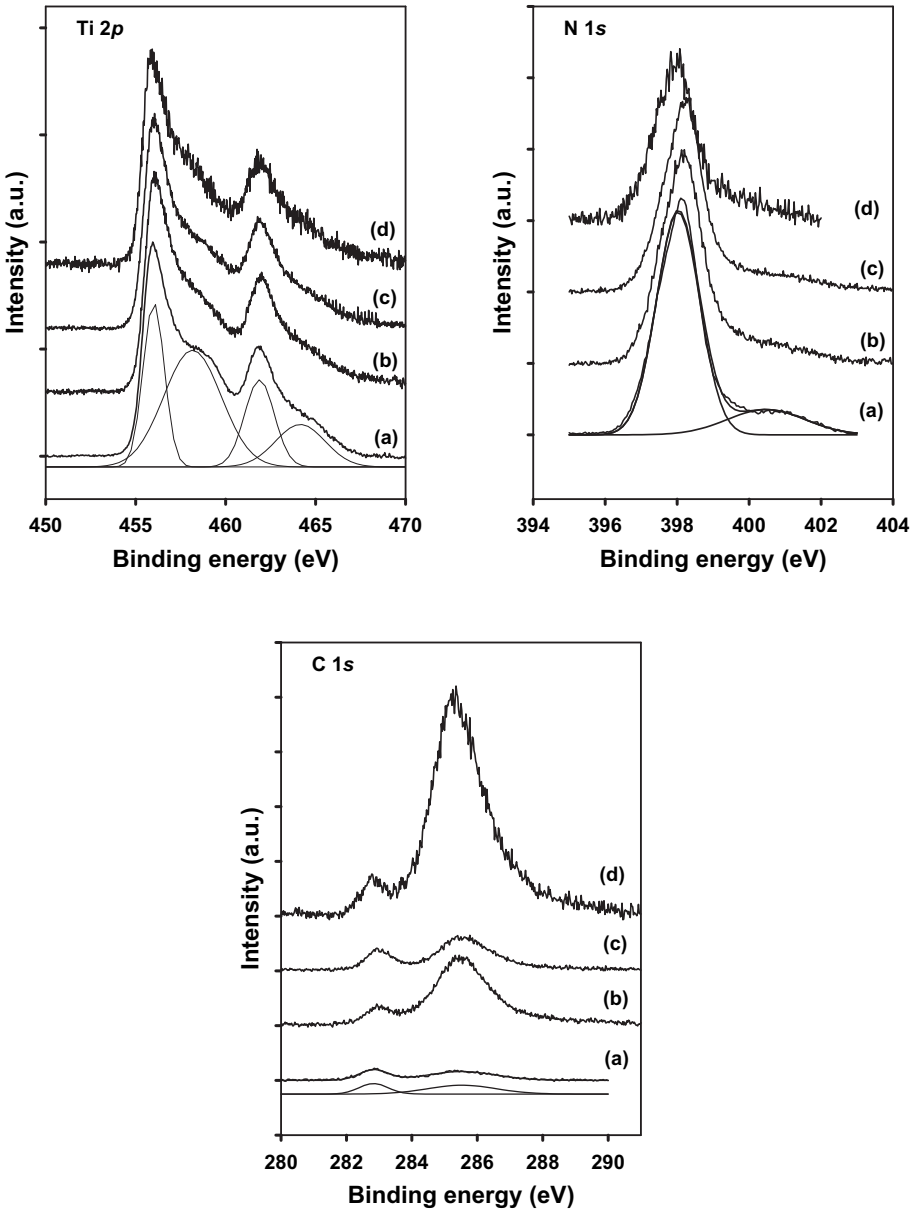

Fig. 3. High-resolution Ti 2*p*, N 1*s*, and C 1*s* XPS spectra of the TiCN coatings deposited from gases with CH_4 fraction of (a) 5, (b) 10, (c) 20, and (d) 30%.

affect the coating's mechanical and wear properties. The high fraction absorbed amorphous carbon in the coatings explains the high defect density in the TiCN coatings. The area of the second peak was used during the calculation of the coating composition.

To investigate the crystalline structure of the TiN and TiCN coatings, XRD was used. Fig. 4 depicts the deposited (a) TiN, (b) Ti5CN, (c) Ti10CN, (d) Ti20CN, and (e) Ti50CN coatings on 17-4 stainless steel substrates. 4 peaks corresponding to the (111), (200), (220), and (222) plane of the cubic TiN phase were observed in the XRD patterns of the TiN coatings. The high intensity of the TiN (111) peak indicates that the deposited TiN coatings grow preferentially along (111) orientation. In addition, one weak peak originating from Ti (101) plane was also observed. This peak is attributed to the Ti bonding layer underneath the TiN top layer. After adding 5% of CH_4 gas into the chamber, a significant reduction in the intensity of the TiN (111) peak and an increase in the intensity of the TiN (220) peak were seen, indicating a change in the preferred orientation from (111) to (220). However, for the coatings deposited with a CH_4 fraction of above 20%, the relative intensity of the (111) peaks increases, and the coating still exhibits a slight (220) preferred orientation. No diffraction peaks originating from TiC phases are observed from the XRD patterns.

To quantify the influence of the C content in the coatings on the XRD patterns, the TiN (220) peaks were fitted using Gaussian functions. The fitting results are shown in Fig. 5. A variation trend of down shifting of the TiN (220) peak with increasing C content in the coatings was observed. The d-values for the TiN (220) plane of the TiCN coatings with different C content were also calculated using Bragg's law [19], $(1/d_{hkl}) = (2/\lambda)\sin\theta$, where d_{hkl}, λ, and θ are interplanar spacing of the (hkl) plane, wavelength of the X-ray, and half of the diffraction angle, respectively. The calculated results were also included in Fig. 5. A gradual increase in the d-spacing with increasing C content in the coatings was observed. It was reported that TiCN lattice parameters exhibit values between the TiN and TiC lattice parameters which are related to the carbon content. As TiCN coating is a solid solution of C atoms in TiN crystal

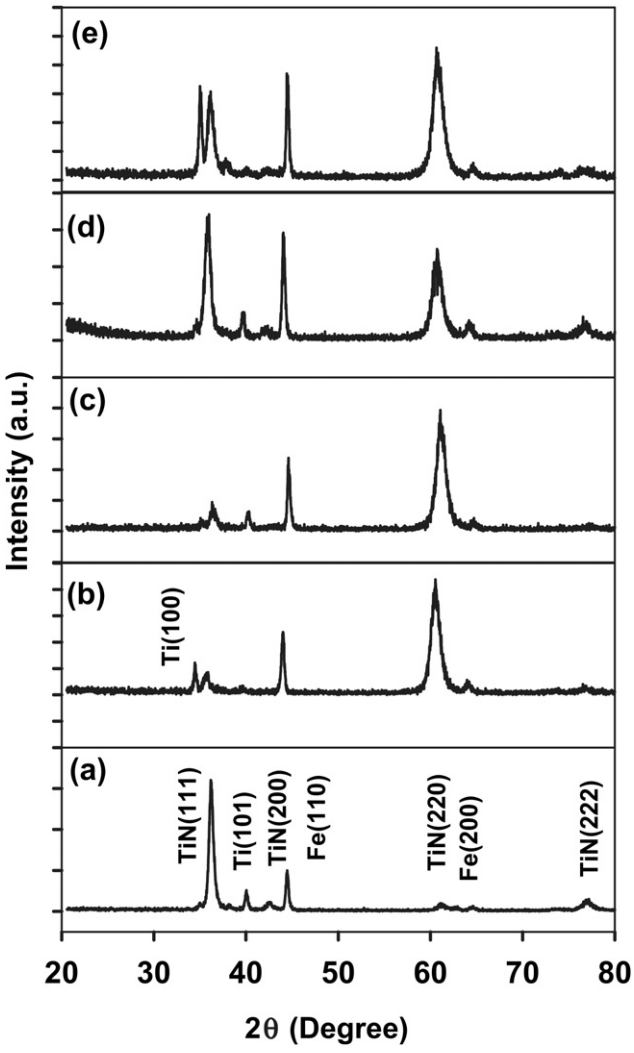

Fig. 4. XRD patterns of the (a) TiN, (b) Ti5CN, (c) Ti10CN, (d) Ti20CN, and (e) Ti50CN coatings deposited LAFAD.

lattice, the large size of C atoms when compared with N atoms causes a distortion of the lattice, and therefore, the increase in the d-value. Typically, the lattice parameter increases with increasing C content in the TiCN coating.

Fig. 5(b) depicts the FWHM of the TiN (220) peak. Clearly, an increase in the C content in the coatings leads to a linearly increase

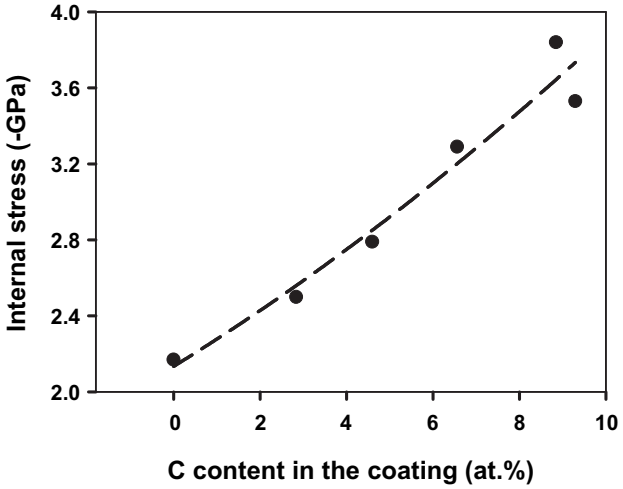

Fig. 6. Internal stress in the TiCN coatings as a function of the C content in the coatings.

in the FWHM of the TiN (220) peak. The grain size was computed using the Scherer equation [19]:

$$D = \frac{0.9\,\lambda}{B\cos\theta}$$

where D is the diameter of the grain, B is the FWHM of the diffraction peak, and θ is half of the diffraction angle. The calculated grain sizes for TiCN coatings with different C content were also included in Fig. 5(b). As shown, with increasing C content from 0 to 9.3 at.%, the TiN grain size decreases linear from 8.9 to 6.6 nm.

The internal stress of the TiCN coatings was also measured using the substrate bending method. Fig. 6 shows the dependence of the internal stress in the TiCN coatings on the C content in the coatings. The C content was measured using XPS. We observe that all the TiCN coatings deposited by LAFAD technique exhibit compressive stress, and the internal stress in the TiCN coatings increases linearly from 2.2 to 3.8 GPa with increasing C content in the coatings from 0 to 9.3 at.%. As shown in Fig. 5(b), with increasing C content in the coatings, the grain size decreases linearly, indicating the increase in the defect density in the TiCN coatings, corresponding to an increase in the internal stress. In addition, as C atoms have larger atomic radius, the substitution of N atoms with C atoms in the TiCN coatings causes the expansion of the lattice spacing. However, the coatings were confined by the substrate. As a result, the substrate exerts a compressive stress to the coatings. With the increase in the C content in the coatings, the degree of expansion of the lattice spacing increases, corresponding to a linearly increase in the internal stress in the coatings.

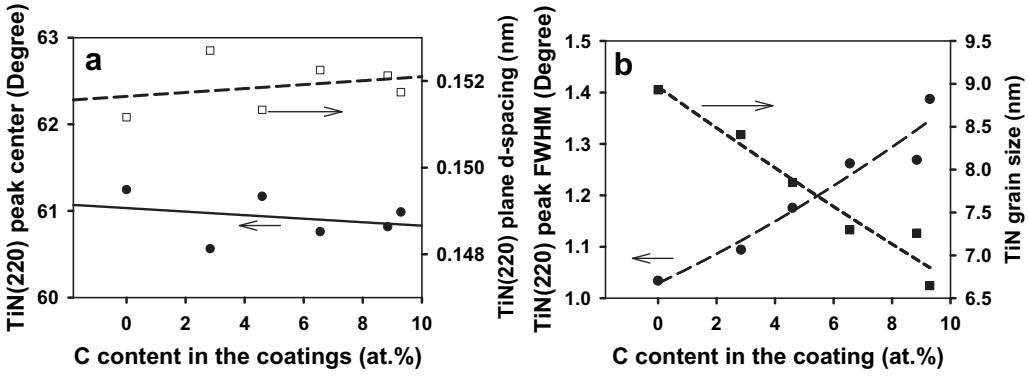

Fig. 5. Influence of the C content in the coatings on the (a) center and FWHM of the TiN (220) peaks and the calculated TiN grain size.

4. Conclusion

TiCN coatings with different C content were deposited by using LAFAD technique using Ti targets under the atmosphere of mixed N_2 and CH_4 gases with CH_4 fraction between 0 and 50%. The surface morphology, composition, bonding structure, and crystalline structure of the deposited coatings were investigated by SEM, XPS, and XRD. The internal stress in the coatings was measured by a substrate bending method. SEM results show that the TiCN coatings consist of nano-sized clusters, and the cluster size increases with increasing CH_4 fraction. XPS results show that with increasing CH_4 fraction from 0 to 30% the C content in the coatings increase but the N content decreases. The further increase in the CH_4 fraction to 50% results in a slight decrease in the C and N contents in the coatings. In addition, XPS results indicates the existence of Ti–N, Ti–C, Ti–O, C–N, and Ti–O–C bonds in the TiCN coatings; and the Ti–N bonding content decreases and the Ti–C and C–N bonding contents increase with increasing C content in the coatings. XRD results demonstrate that increasing CH_4 fraction in the gases result in a change in the growth orientation of the TiCN coatings from (111) to (220) preferred orientation with the shift of the TiN (220) peak center to a lower diffraction angle, as well as the decreases in the grain size. Substrate bending method shows that with increasing C content in the coatings from 0 to 9.3 at.%, the internal stress in the TiCN coatings increases continuously from 2.2 to 3.8 GPa.

Acknowledgments

The authors would like to express gratitude for the support of The United States Army Telemedicine and Advanced Technology Research Center (TATRC), U.S. Army Medical Research & Material Commandunder contract number of W81XWH-08-2-0023.

References

[1] Knotek O, Loffler F, Kramer G. Surf Coat Technol 1993;61:320.
[2] Guu YY, Lin JF. Wear 1997;210:245.
[3] Hsieh JH, Tan ALK, Zeng XT. Surf Coat Technol 2006;201:4094.
[4] Baravian G, Sultan G, Damond E, Detour H. Surf Coat Technol 1995;76/77:687.
[5] Gergmann E, Kaufmann H, Schmid R, Vogel J. Surf Coat Technol 1990;42:237.
[6] Larsson A, Ruppi S. Thin Solid Films 2002;402:203.
[7] Agudelo LC, Ospina R, Castillo HA, Devia A. Phys Scr T 2008;131:014006.
[8] Senna LF, Achete CA, Hirsch T, Freire Jr FL. Surf Coat Technol 1997;94–95:390.
[9] Hsieh JH, Wu W, Li C, Yu CH, Tan BH. Surf Coat Technol 2003;163/164:233.
[10] Lackner JM, Waldhauser W, Ebner R. Surf Coat Technol 2004;188–189:519.
[11] Karlsson L, Hultman L, Sundgren JE. Thin Solid Films 2000;371:167.
[12] Huang SW, Ng MW, Samandi M, Brandt M. Wear 2002;252:566.
[13] Cheng YH, Browne T, Heckerman B. J Vac Sci Technol A 2010;28(3):431.
[14] Deng J, Braun M, Gudowska I. J Vac Sci Technol A 1994;12:733.
[15] Cheng YH, Browne T, Heckman B, Jiang JC, Meletis EI, Bowman C, et al. J Appl Phys 2008;104:093502.
[16] Mezin A. Surf Coat Technol 2006;200:5259.
[17] Cheng YH, Browne T, Heckman B. J Vac Sci Technol A 2009;27:82.
[18] Guemmaz M, Moraitis G, Mosser A, Khan MA, Parlebas JC. J Phys Condens Matter 1997;9:8453.
[19] Klug HP, Alexander LE. X-ray diffraction procedures for polycrystalline and amorphous materials. New York: Wiley-Interscience; 1974.